

# Infrared emission-line galaxies associated with damped $\text{Ly}_\alpha$ and strong metal absorber redshifts <sup>1</sup>

F. Mannucci

C.A.I.S.M.I.–C.N.R., Florence, Italy

Electronic mail: filippo@arcetri.astro.it

D. Thompson & S. V. W. Beckwith

Max-Planck-Institut für Astronomie, Heidelberg, Germany

Electronic mail: djt@mpia-hd.mpg.de, svwb@mpia-hd.mpg.de

and

G. M. Williger

Goddard Space Flight Center, Greenbelt, MD

Electronic mail: williger@tejut.gsfc.nasa.gov

## ABSTRACT

Eighteen candidates for emission line galaxies were discovered in a narrow-band infrared survey that targeted the redshifts of damped  $\text{Ly}_\alpha$  or metal lines in the spectra of quasars. The presence of emission lines is inferred from the photometric magnitudes in narrow and broad band interference filters, corresponding to  $\text{H}_\alpha$  at redshifts of 0.89 (6 objects) and 2.4 (10 objects), and  $[\text{OII}]\lambda 3727$  at a redshift of 2.3 (2 objects). Most of the candidates are small resolved objects, compatible with galaxies at the redshifts of the absorbers. Because a similar survey targeted at the redshifts of quasars themselves uncovered only one emission-line galaxy in a larger volume, the results imply substantial clustering of young galaxies or formation within filaments or sheets whose locations are indicated by the redshifts of absorption along the lines of sight to more distant quasars.

*Subject headings:* cosmology: observations — early universe — galaxies: formation — infrared: galaxies

---

<sup>1</sup>Based on observations collected with the DSAZ telescopes in Calar Alto and ESO telescopes in La Silla

## 1. Introduction

Exploration of the high redshift universe and discovery of the most distant objects is still in its infancy. Only recently have the tools been available to detect normal galaxies at redshifts larger than one, when the first galaxies were created (Pascarella, Windhorst, & Odewahn 1996, Hu & McMahon 1996, Cowie & Hu 1998, Steidel et al. 1996). It seems likely that young galaxies will have a variety of different signatures so that it will be necessary to use several diverse techniques to uncover all of them: searches at optical, infrared, x-ray, and radio wavelengths, for example. In particular, basing the statistical studies of the high redshift galaxies only on objects detected in the rest-frame UV could miss many young galaxies (Franceschini et al. 1998, Guiderdoni et al. 1997), and sampling longer wavelength ranges is necessary.

We carried out a survey for infrared emission-line galaxies by imaging through narrow ( $\frac{\Delta\lambda}{\lambda} \sim 0.01$ ) and broad band filters between 1 and  $2.5 \mu\text{m}$ , identifying objects that appeared brighter in the narrow filters (Thompson, Mannucci, & Beckwith 1996, hereafter TMB96). Our first survey was designed to uncover emission lines at the redshifts of quasars within each survey field, in case there is substantial clustering marked by quasars. In an area of  $276 \square'$ , only one emission-line galaxy was discovered (Beckwith et al. 1998). The surface density of such objects implied by these results is similar to that inferred from other surveys (Cowie et al. 1994, Graham & Dey 1996, Malkan, Teplitz, & McLean 1996, Bechtold et al. 1997) and suggests that the infrared emission-line galaxies constitute at most a modest population of young galaxies at high redshift.

Using the same instruments, we undertook a second infrared survey for emission-line galaxies targeted at the redshifts of damped  $\text{Ly}_\alpha$  or metal absorption lines in the spectra of quasars. Damped  $\text{Ly}_\alpha$  absorbers are thought to contain as much baryonic matter as seen in all spiral galaxies today (Wolfe et al. 1986) and may, therefore, mark sites of ongoing star formation. Several other groups (Lowenthal et al. 1991, Macchetto et al. 1993, Wolfe et al. 1992, Møller & Warren 1993, Djorgovski et al. 1996, Francis, Woodgate, & Danks 1997) carried out similar surveys at optical wavelengths looking for  $\text{Ly}_\alpha$  emission-line galaxies in these regions. They discovered only a few such emission-line (non-AGN) galaxies, but Wolfe 1993 showed that the implied volume density was significantly higher than in the general field. Metal absorption systems also indicate that star formation has taken place, and are identifiable from the ground at lower redshifts than  $\text{Ly}_\alpha$  alone.

We selected damped  $\text{Ly}_\alpha$  systems or metal absorbers whose redshifts put the main optical lines  $\text{H}_\alpha$ ,  $\text{H}_\beta$ , [OIII], and [OII] into standard narrow-band filters in the J, H and K bands. The resulting redshift ranges are:  $0.5 < z < 1.9$ ,  $2.1 < z < 2.5$  and  $3.1 < z < 3.8$ . Special emphasis was given to the  $\text{H}_\alpha$  line expected to be the brightest in young star systems and the least affected by dust. This letter describes the results of the new survey.

## 2. Observations

As described in TMB96, pairs of narrow and broad-band images were taken of the selected fields. Most of the data,  $163 \square'$  in 13 fields, were obtained at the Calar Alto 3.5m telescope, using the NICMOS3 256<sup>2</sup> MAGIC cameras (Herbst et al. 1993) with a resolution of  $0''.81$  per pixel. One field,  $38.6 \square'$ , was obtained at the same telescope with the Omega Prime camera using a 1024<sup>2</sup>, HgCdTe Hawaii array with  $0''.40$  per pixel. Five more fields for a total of  $26.2 \square'$  were observed with the IRAC2b camera at the 2.2m ESO/MPI telescope at La Silla. The area-weighted average limiting flux is  $2.4 \times 10^{-16} \text{ erg cm}^{-2} \text{ sec}^{-1}$ , or  $1.6 \times 10^{-16} \text{ erg cm}^{-2} \text{ sec}^{-1}$ , if only the Calar Alto data are considered. The comoving volume sampled by this survey at the redshift of the absorbers is about  $20,600 \text{ Mpc}^3$ , assuming only the target line at the appropriate redshift could be detected. Considering all the four principal optical lines [OII],  $H_\beta$ , [OIII] and  $H_\alpha$ , the total sampled volume is  $90,000 \text{ Mpc}^3$  ( $H_0 = 50$ ,  $q_0 = 0.5$ , assumed throughout this paper). For comparison, the total sampled volume by the first survey targeting quasars redshifts is  $153,000 \text{ Mpc}^3$ .

## 3. Results

Objects were selected if well detected in the narrow-band images, with narrow-band magnitudes exceeding the broad-band magnitudes by more than 2.5 standard deviations of the combined uncertainties in the two filters, and with derived line equivalent width larger than  $50 \text{ \AA}$ . These criteria are easily checked by plotting objects in a color-magnitude diagram, where the color is the broad minus narrow band magnitude. Figure 1 is a color-magnitude diagram of the Q0100+130 (PHL 957) field showing the detection of two candidates discovered in the J band. The candidates, denoted A & B, clearly stand out above the noise at high equivalent width, although A is near the narrow-band limit. This field also contains a  $\text{Ly}_\alpha$  emission-line galaxy discovered by Lowenthal et al. 1991 and subsequently imaged in the  $H_\alpha + [\text{NII}]$  lines at  $2.177 \mu\text{m}$  by Bunker et al. 1995. This object is not seen in our image, and its expected [OII] $\lambda 3727$  flux (about  $0.7 \times 10^{-16} \text{ cgs}$ ) derived from the  $H_\alpha$  flux by Bunker et al. 1995 is below our detection threshold (about  $1.4 \times 10^{-16} \text{ cgs}$ ). Neither A nor B is seen in the Lowenthal et al. 1991 image, while our candidate A is barely visible on the Bunker et al. 1995 narrow band image, implying faint  $H_\alpha$  emission. Both A and B are visible in their broad band K image, as well, thus supporting the reality of the detections in our survey.

From the color-magnitude diagrams of five of the 19 fields in this survey, we discovered 18 candidates for emission-line galaxies. The emission lines, if spectroscopically confirmed, would correspond to  $H_\alpha$  at redshifts of 0.89 (6 objects) and 2.4 (10 objects), or [OII] $\lambda 3727$  at a redshift of 2.3 (2 objects). Most of the objects are a few seconds of arc in extent suggesting that they are galaxies at redshifts greater than a few tenths.

Table 1 lists the coordinates of the candidates, their offsets from the quasar, and their morphology as deduced from our images. The angular distances from the quasars are between

9" and 120", corresponding to projected distances between 70 kpc and 1 Mpc at the distances to the absorption-line systems. Very few, if any, of these objects could, therefore, be identified with the absorption-line objects, whose typical extents are probably those of galaxies or protogalactic clumps,  $\sim 5 - 60$  kpc across (Fukugita, Hogan, & Peebles 1996, Haehnelt, Steinmetz, & Rauch 1996). However, due to the coarse sampling in our images, no attempt was made yet to subtract a PSF from the QSO image, so objects within a few arcsec from the QSO would not have been easily seen.

Table 2 gives the magnitude, a rank of the significance of the detection, the statistical signal-to-noise ratio of the emission line, and the line flux for each candidate. The final four columns give the line identification, redshift, rest equivalent width, and derived star formation rate (Mannucci & Beckwith 1995; TMB96) assuming the line is at the redshift of the absorption-line. The derived SFRs attribute all of the line emission to HII regions, ignoring any contribution from an active galactic nucleus (AGN), an assumption that may be incorrect in at least some cases (Beckwith et al. 1998).

Figure 2 shows images of each candidate in the narrow and broad filters. The typical angular resolution is about  $1''.2$ , corresponding to about  $\sim 10$  kpc for redshifts between 1 and 3. Most of the objects appear resolved even at this resolution. The field around Q1623+268 was observed by Steidel in 1996 May with the Hubble Space Telescope using the WFPC2 camera with the F702W filter and total integration time of 87 min. Two of our emission-line candidates, Q1623+268A and Q1623+268D, appear in these images, parts of which are shown in Figure 3. Both objects appear to be late-type spiral or irregular galaxies. The object sizes are  $2''.4$  (Q1623+268A) and  $3''.6$  (Q1623+268D), corresponding to 20 and 30 Kpc for  $z \simeq 0.9$ . If these objects are at the assumed redshifts, they are large, well formed galaxies. The detected star formation activity with SFRs between 5 and 10  $M_{\odot}/\text{yr}$  would be the normal activity of late-type spiral or irregular galaxies.

#### 4. Discussion

The most striking result of this survey is the large number of candidates discovered in a small area implying that by choosing the right redshift intervals, it is possible to detect emission-line objects rather easily. The total sky coverage in this survey was  $228 \square'$  compared with  $276 \square'$  in TMB96, yet 18 candidates were discovered in the second survey compared to a single emission-line galaxy in the first. Taken at face value, the new results suggest that damped  $\text{Ly}_{\alpha}$  and metal absorbers pinpoint the regions where galaxy formation is taking place.

Confirmation of the exact nature of these objects will require spectroscopic follow up and perhaps additional imaging with HST. Since not all the objects are resolved at the coarse pixel scale used, some could be stars or other nearby objects. A few objects are near the  $3\sigma$  detection limit. Statistical comparison must, therefore, be regarded with some caution until further data are available.

Nevertheless, we believe that the main result of this survey is robust: there are more emission-line galaxies associated with damped  $\text{Ly}_\alpha$  and metal absorber redshifts than with the redshifts of quasars or at arbitrary redshifts. First, the observational method employed was identical to that of TMB96, but the resulting number of candidates is almost 20 times larger. Second, the one candidate, cK39, discovered in the first survey by TMB96 was also coarsely sampled but is, indeed, an emission line galaxy (Beckwith et al. 1998) spectroscopically confirmed and easily resolved with the Keck telescope. Third, the HST images of two of our *least* statistically significant candidates show them to be galaxies of exactly the size expected for objects at redshifts greater than a few tenths and with the kind of morphology expected of objects in late stages of assembly.

These results may be compared with similar studies of  $\text{Ly}_\alpha$  emitting galaxies in the neighborhood of damped  $\text{Ly}_\alpha$  absorption line systems. By the number of detected objects (Lowenthal et al. 1991, Wolfe et al. 1992, Macchetto et al. 1993, Møller & Warren 1993, Djorgovski et al. 1996) and observed fields (Smith et al. 1989, Deharven, Buat, & Bowyer 1990, Lowenthal et al. 1995) an average comoving density of these systems of about  $7 \times 10^{-4} \text{ Mpc}^{-3}$  is derived down to a limiting SFR of about  $5 \text{ M}_\odot/\text{yr}$ , assuming case B recombination and no dust. The infrared technique gives similar results, i.e., detections in about 1/4 of the fields and a density of  $9 \times 10^{-4} \text{ Mpc}^{-3}$ . The range of SFR implied by our observations 6 - 200  $\text{M}_\odot/\text{yr}$ , is somewhat higher than that usually obtained by the optical searches, 5 - 20  $\text{M}_\odot/\text{yr}$ , but not dramatically so. If there is modest local extinction to the star formation regions in high redshift galaxies, optical derived SFRs must be increased by a factors of about 3 to get the true SFR (Pettini et al. 1998), making their range almost coincident with ours. Our results are perhaps more consistent with the limiting SFR of 30 - 80  $\text{M}_\odot/\text{yr}$  along sightlines toward eight  $z > 2$  damped  $\text{Ly}_\alpha$  absorbers as derived from redshifted  $\text{H}\alpha$  (Bunker et al. 1998).

On the other hand, the lines could be produced by active galactic nuclei. There are several good reasons to believe this could be the case for the one emission-line object discovered in the survey of TMB96 (Beckwith et al. 1998), and that it could be a widespread phenomenon (Francis, Woodgate, & Danks 1997). If so, the density of such objects in these regions is considerably higher than the cosmic average. The density of known quasars at these redshifts (e.g., Andreani & Cristiani 1992) implies about  $4 - 8 \times 10^{-5}$  quasars per field, meaning that we might be seeing far more AGNs than expected. Although the damped  $\text{Ly}_\alpha$  redshifts mark regions with many galaxies, the nature of each single galaxy will remain a mystery until proper follow up observations will be able to distinguish between emission due to star formation and AGNs.

Cold dark matter simulations of early galaxy formation produce filaments of galaxies (White 1994) with groups of high redshift metal and damped  $\text{Ly}_\alpha$  absorbers spanning up to several hundred kpc (Rauch, Haehnelt, & Steinmetz 1997). If the damped  $\text{Ly}_\alpha$  absorbers actually trace the positions of these filaments, then the high detection rate of emission line galaxies in this survey may support the overall structure predicted by CDM. This conclusion can be made quantitative by measuring the average overdensity of objects near damped  $\text{Ly}_\alpha$  and metal systems with respect

to TMB96.

We are grateful to the staffs at the Calar Alto Observatory and ESO at La Silla for excellent assistance with the observations. We profited from discussions with Esther Hu, Garth Illingworth, Matt Malkan, Ed Salpeter and Chuck Steidel. This research was supported by the Max-Planck-Society and also uses Archival data from the Hubble Space Telescope. FM acknowledges partial support by ASI grant ARS-96-66.

## REFERENCES

- Andreani, P., & Cristiani, S. 1992, *ApJ*, 398, L17
- Bechtold, J., Yee, H. K. C., Elston, R., & Ellingson, E. 1997, *ApJ*, 477, L29
- Beckwith, S. V. W., Thompson, D. J., Mannucci, F., & Djorgovski, S. G. 1998, *ApJ*, in press
- Bunker, A. J., Warren, S. J., Hewett, P. C., & Clements, D. L. 1995, *MNRAS*, 273, 513
- Bunker, A. J., Warren, S. J., Clements, D. L., Williger, G. M., & Hewett, P. C. 1998, preprint
- Cowie, L. L., & Hu, E. M. 1998, *AJ*, in press (astro-ph/9801003)
- Cowie, L. L., Songaila, A., Hu, E. M., Egami, , Huang, J.-S., Pickles, A. J., Ridgway, S. E., & Wainscoat, R. J. 1994, *ApJ*, 432, L83
- Deharveng, J. M., Buat, V., & Bowyer, S. 1990, *Å*, 236, 351
- Djorgovski, S. G., Pahre, M. A., Bechtold J., & Elston, R. 1996, *Nature*, 382, 234
- Franceschini, A., Silva, L., Granato, G. L., Bressan, A., Danese, L. 1998, *ApJ*, in press
- Francis, P. J., Woodgate, B. E., & Danks, A. C. 1997, *ApJ*, 482, 25
- Fukugita, M., Hogan C.J., Peebles P.J.E. 1996, *Nature*, 381, 489
- Graham, J. R., & Dey, A. 1996, *ApJ*, 471, 720
- Guideroni, B., Bouchet, F. R., Puget, J.-L., Lagache, G., & Hivon, E. 1997, "The optically dark side of galaxy formation" *Nature*, 390, 257
- Haehnelt, M.G., Steinmetz, M., & Rauch, M. 1996, *ApJ*, 465, L95

- Herbst, T. M., Beckwith, S. V. W., Birk, Ch., Hippler, S., McCaughrean, M. J., Mannucci, F., & Wolf, J. 1993, in *Infrared Detectors and Instrumentation*, SPIE Conference 1946, Fowler, A. M. (ed.), p. 605
- Hu, E. M., McMahon, R. G. 1996, *Nature*, 382, 231
- Lowenthal, J. D., Hogan, C. J., Green, R. F., Caulet, A., Woodgate, B. E., Brown, L., and Foltz, C. B. 1991, *ApJ*, 377, L73
- Lowenthal, J.D. et al., 1995, *ApJ*, 451, 484
- Macchetto, F., Lipari, S., Giavalisco, M., Turshek, D. A., & Sparks, W. B. 1993, *ApJ*404, 511
- Malkan, M. A., Teplitz, H., & McLean, I. S. 1996, *ApJ*, 468, L9
- Mannucci, F., & Beckwith, S. V. W. 1995. *ApJ*, 442, 569
- Møller, P., & Warren, S. J. 1993, *å*, 270, 43
- Pascarelle, S. M., Windhorst, R. A., & Odewahn, S. C. 1996, *Nature*, 383, 45
- Pettini, M., Steidel, C. C., Adelberger, K. L, Kellogg, M., Dickinson, M., & Giavalisco, M. 1998, *astro-ph/9708117*
- Rauch, M., Haehnelt, M. G., & Steinmetz, M. 1997, *ApJ*, 481, 624
- Smith, H. E., Cohen, R. D., Burns, J. E., Moore, D. J., & Uchida, B. A. 1989, *ApJ*, 347, 87
- Steidel, C. C., Giavalisco, M., Pettini, M., Dickinson, M., & Adelberger, K. L. 1996, *ApJ*, 462, 17
- Thompson, D. J, Mannucci, F., & Beckwith, S. V. W. 1996, *AJ*, 112, 1794
- White, S. D. M. 1994, *MPA preprint*, # 831.
- Wolfe, A. M. 1993, *ApJ*, 402, 411
- Wolfe, A. M.,Turnshek, D. A., Lanzetta, K. M., & Oke, J. B. 1992, *ApJ*, 385, 151
- Wolfe, A. M., Turnshek, D. A., Smith, H. E., & Cohen, R. E. 1986, *ApJS*, 61, 249

Table 1. The Emission-line Candidates

Object	RA(2000)	DEC(2000)	$\Delta^a$ ( $''$ )	$D^b$ ( $''$ )	P.A. <sup>b</sup> (deg.)	Size <sup>c</sup> ( $''$ )	Shape
Q0100+130A	01:03:10.39	+13 17 03.7	1.1	48	344.3	5.4×1.5	possibly double
Q0100+130B	01:03:13.30	+13 16 58.7	0.5	51	35.3	1.9×1.2	unresolved
Q0201+365A	02:04:56.28	+36 49 14.9	0.5	9	112.6	<sup>d</sup>	unresolved
Q0201+365B	02:04:56.86	+36 50 02.2	0.5	46	18.9	1.8×1.8	resolved
Q0201+365C	02:04:50.20	+36 47 47.4	0.5	112	215.6	2.4×1.4	resolved
Q0201+365D	02:05:01.75	+36 47 47.0	0.5	117	141.0	1.4×1.2	core/asymm. halo
Q1623+268A	16:25:48.56	+26 47 07.9	0.5	9	340.9	1.6×1.0	resolved
Q1623+268B	16:25:51.30	+26 47 21.1	0.5	40	56.7	3.8×2.2	irregular, diffuse
Q1623+268C	16:25:51.62	+26 48 17.2	0.5	87	25.9	2.5×2.5	irregular
Q1623+268D	16:25:43.39	+26 45 40.9	0.5	106	222.8	2.9×1.8	faint, elongated
Q1623+268E <sup>e</sup>	16:25:56.69	+26 46 08.1	0.5	117	115.6	1.1×1.1	faint, unresolved
Q1623+268F <sup>e</sup>	16:25:56.42	+26 46 06.1	0.5	152	117.3	1.8×1.0	core/asymm. halo
Q2038–012A	20:40:52.99	–01 05 29.2	0.7	25	69.6	2.5×1.5	elongated
Q2038–012B	20:40:47.62	–01 07 15.8	0.7	113	210.0	1.5×1.5	diffuse
Q2038–012C	20:40:53.61	–01 07 32.6	0.7	119	163.7	2.2×1.2	irregular
Q2038–012D	20:40:57.93	–01 06 50.8	0.7	122	126.5	1.3×1.2	unresolved
Q2348–011A	23:50:57.29	–00 52 02.5	0.7	11	225.6	<sup>d</sup>	unresolved
Q2348–011B	23:50:54.64	–00 52 58.4	0.7	68	315.6	1.6×1.2	faint, elongated

<sup>a</sup>Radial uncertainty in the position

<sup>b</sup>Projected distance and position angle (north to east) from the QSO

<sup>c</sup>Object sizes measured by the FWHM along respectively the major and minor axis of elliptical gaussians fitted to the objects

<sup>d</sup>not fitted because of the presence of a nearby object

<sup>e</sup>the distance between objects is only 4 $''$  (33 Kpc); they could be one galaxy



Table 2. Candidate Magnitudes and Derived Properties

Object	$\lambda(\text{NB})$ $\mu\text{m}$	NB (mag)	BB (mag)	R <sup>a</sup>	S/N	Line flux ( $10^{-16}$ cgs)	Line	z	EW <sub>r</sub> ( $\text{\AA}$ )	SFR ( $M_{\odot}/\text{yr}$ )
Q0100+130A	1.237	20.33	21.44	2	3.8	$1.9\pm 0.5$	[OII]	2.31	$75\pm 26$	$198\pm 50$
Q0100+130B	1.237	19.88	20.88	2	5.6	$2.7\pm 0.5$	[OII]	2.31	$63\pm 14$	$283\pm 50$
Q0201+365A <sup>b</sup>	2.248	18.45	19.37	2	4.2	$1.8\pm 0.4$	H $_{\alpha}$	2.42	$65\pm 20$	$68\pm 16$
Q0201+365B	2.248	18.55	19.62	2	4.3	$1.8\pm 0.4$	H $_{\alpha}$	2.42	$88\pm 27$	$71\pm 16$
Q0201+365C	2.248	18.92	>20.78	2	4.2	$1.9\pm 0.4$	H $_{\alpha}$	2.42	>182	58–92
Q0201+365D	2.248	18.71	20.12	1	4.5	$2.0\pm 0.4$	H $_{\alpha}$	2.42	$158\pm 62$	$76\pm 16$
Q1623+268A	1.237	20.47	21.35	1	2.6	$1.4\pm 0.6$	H $_{\alpha}$	0.89	$91\pm 49$	$6\pm 3$
Q1623+268B	1.237	19.96	20.98	2	4.5	$2.5\pm 0.6$	H $_{\alpha}$	0.89	$115\pm 37$	$10\pm 3$
Q1623+268C	1.237	20.24	>22.18	2	4.6	$2.7\pm 0.3$	H $_{\alpha}$	0.89	>248	8–14
Q1623+268D	1.237	20.40	21.29	3	2.8	$1.5\pm 0.6$	H $_{\alpha}$	0.89	$92\pm 47$	$6\pm 3$
Q1623+268E	1.237	20.42	>22.18	3	3.7	$2.1\pm 0.6$	H $_{\alpha}$	0.89	>180	6–12
Q1623+268F	1.237	20.50	21.40	3	2.6	$1.4\pm 0.6$	H $_{\alpha}$	0.89	$94\pm 51$	$6\pm 3$
Q2038–012A	2.248	18.09	18.77	2	3.5	$1.7\pm 0.4$	H $_{\alpha}$	2.42	$37\pm 10$	$68\pm 16$
Q2038–012B	2.248	19.01	20.73	2	3.3	$1.7\pm 0.4$	H $_{\alpha}$	2.42	$256\pm 170$	$65\pm 16$
Q2038–012C	2.248	18.44	19.66	1	4.5	$2.3\pm 0.4$	H $_{\alpha}$	2.42	$115\pm 32$	$88\pm 16$
Q2038–012D	2.248	18.90	>20.84	1	3.9	$2.0\pm 0.4$	H $_{\alpha}$	2.42	>194	60–94
Q2348–011A <sup>b</sup>	2.248	18.74	20.27	2	3.0	$2.0\pm 0.6$	H $_{\alpha}$	2.43	$191\pm 95$	$78\pm 21$
Q2348–011B	2.248	18.81	>20.79	3	3.2	$2.2\pm 0.6$	H $_{\alpha}$	2.43	>199	63–107

<sup>a</sup>R rank degree of significance: 1 is highest, 3 is lowest; was estimated by inspection to take into account systematic uncertainties such as a very bright continuum, proximity to the edge of the field, and proximity of nearby objects making accurate magnitudes difficult to derive

<sup>b</sup>Magnitudes may be affected by nearby objects

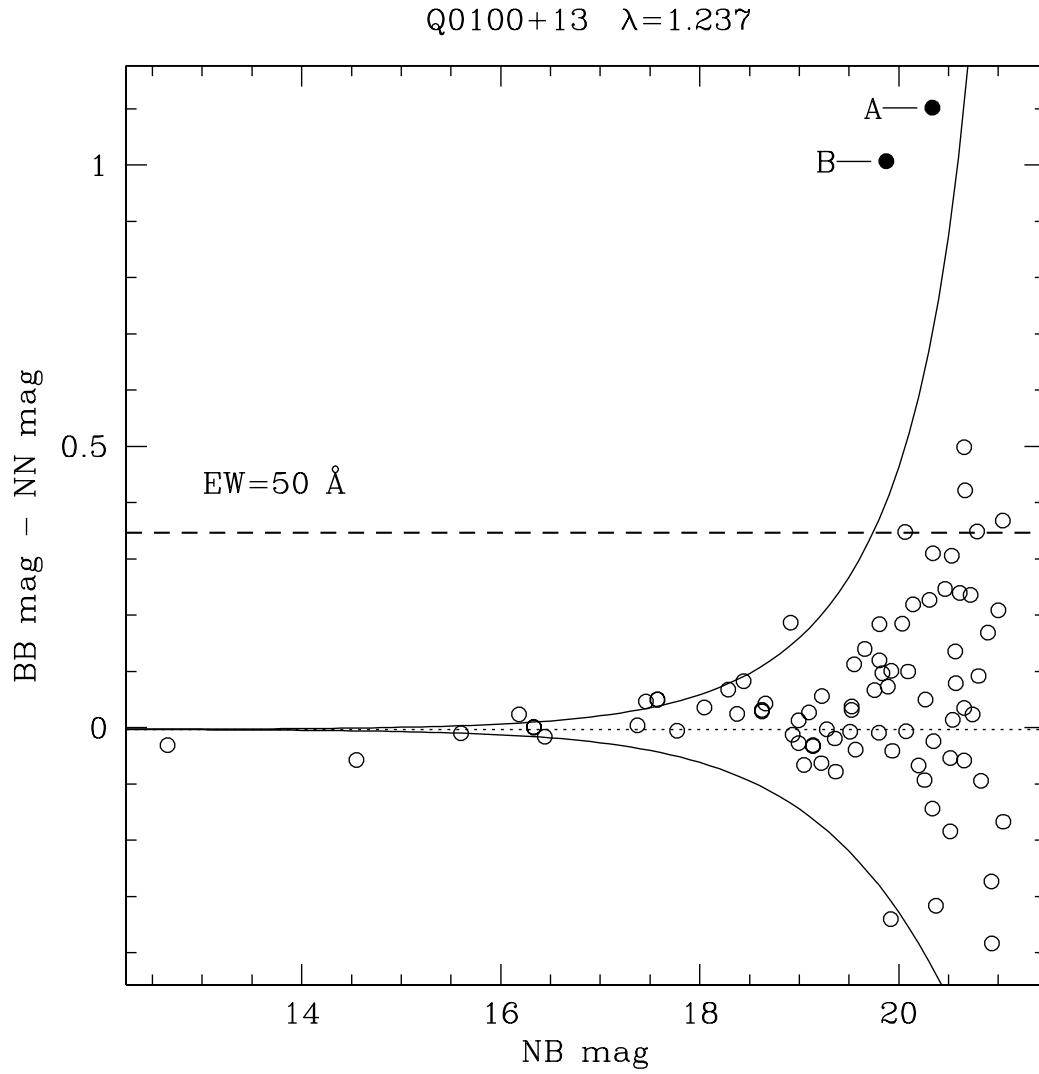


Fig. 1.— Color - magnitude diagram for the Q0100+130 (PHL 957) field. The solid lines indicate the  $3\sigma$  uncertainties, the dashed line shows the position of objects with an emission line with  $EW=50\text{\AA}$ . The two candidate emission-line galaxies are marked as A and B.

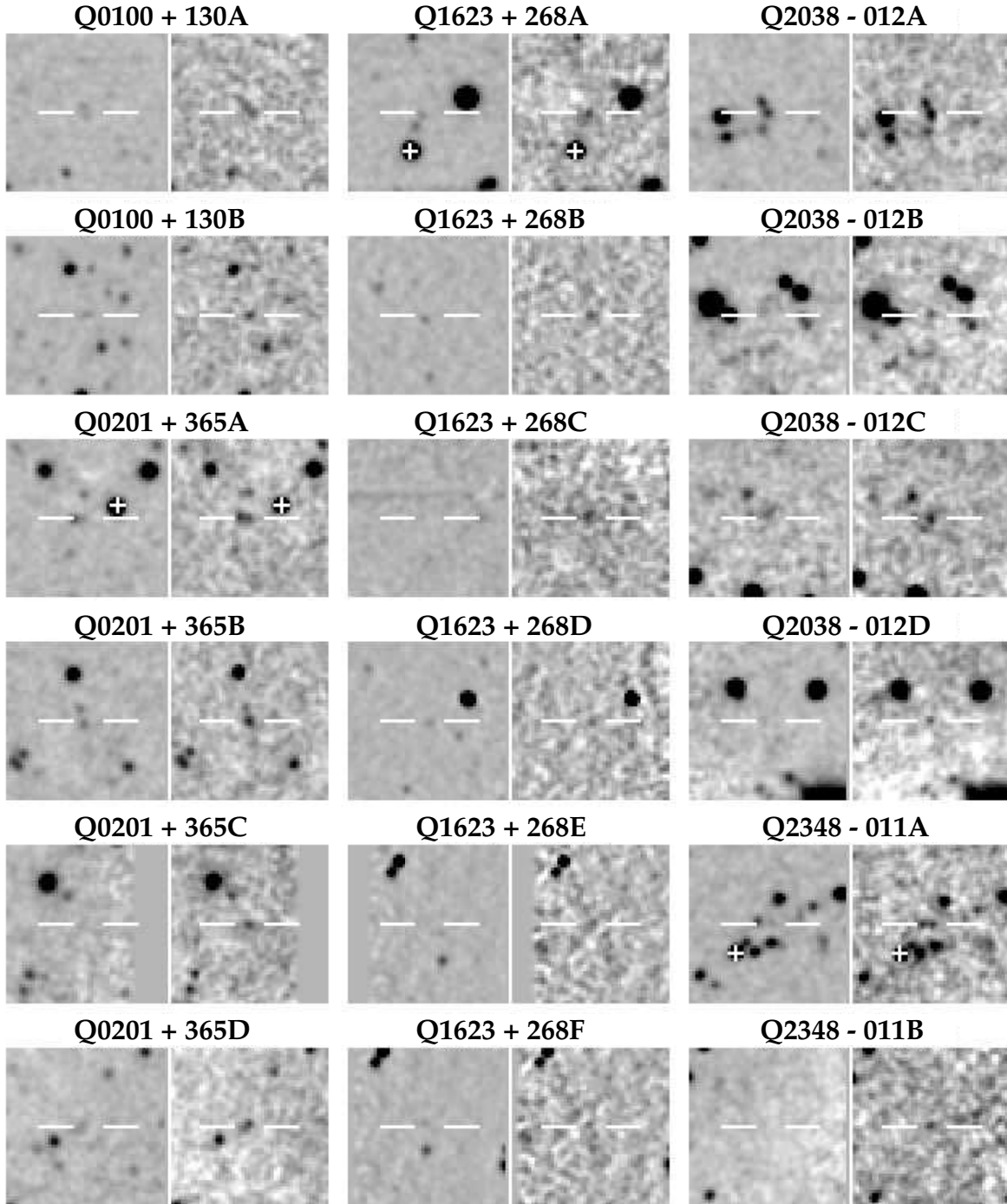


Fig. 2.— Images of the candidates. In each panel, the BB image is on the left and the corresponding NB image on the right, with the candidate at the center. A white cross marks the QSO when present in the field. The images have been convolved with a gaussian with FWHM about equal to the seeing to make the faint objects more visible. The dimensions of each subimage are 40 arcsec, North is up and East left.

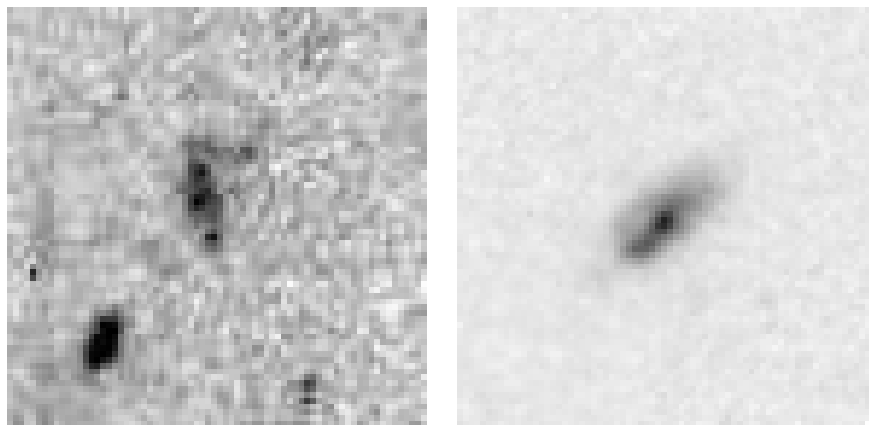


Fig. 3.— HST WFPC2 images of two of the candidates in the Q1623+268 field: A (left) and D (right). The dimensions of each image are 72 pixels or 7.2 arcsec on each side. The images have been rotated from the original WFPC2 orientation so that north is up and east to the left.